Original Research Article

A GIS based mapping of seismic parameters in tectonically active Mikir massif region of Assam, India

ABSTRACT

The Mikir massif area of Assam is considered one of the deformed zones of the north-eastern region (NER) as demonstrated by its seismicity. The present study aims to study the active tectonics in the Mikir massif region with the help of hypocentral parameters, frequency–magnitude relation, and 'b' and 'a' values of earthquake events. The major structures and existing lineaments of the area are correlated with the seismicity pattern and areas having low seismicity and less heterogeneity has been demarcated based on seismic parameters. The seismicity in the area shows a higher concentration of earthquake events towards NW compared to other parts. The depth section of earthquake events along and across the regional faults shows that all the major structures and lineaments with distinct topographic expressions can be identified from the seismic profile. The activeness of those faults and lineaments can be accessed by the cluster of seismic events that occurred spatially and also at depth. Classification of the area into 4 different seismogenic zones shows higher values of seismic parameters (Mc, a, and b) for Zone A, followed by Zone C, Zone B, and Zone D. The higher seismicity associated with these zones is also confirmed by high lineament density in those areas. The lower b and a- value associated with Zone D implies that the area is seismotectonically stable with fewer numbers of seismic events and hence suitable for any civil engineering construction.

Keywords:

Mikir massif, Seismicity, a-value, b-value, NER.

1. Introduction

An earthquake is a major natural threat to mankind killing thousands of people every year with the destruction and collapse of buildings and causing economic losses [1]. Knowledge and visualization of the present-day relationship between earthquakes, active tectonics and crustal deformation is a key to understand the geodynamic processes[2], and is also essential for risk mitigation and the management of any civil engineering project constructed in a tectonically active area. The safety of infrastructures such as buildings, bridges, dams, etc. is of prime importance and should be designed and built to withstand earthquake loads with minimum or no damage. To mitigate the hazard, site-specific seismic hazard analysis should be done in areas showing higher seismicity in the recent past. A reliable seismic hazard assessment could provide the necessary design inputs for earthquake-resistant structures in seismically active regions [1]. Structures that meet the minimum standards should be able to withstand the applied earthquake loads without suffering serious failures that cause them to collapse and result in human fatalities.In terms of seismicity, Northeastern India (NER) is one of the most active regions in the world. The region lies in the most active zone V [3] of the Indian Seismic Code (IS: 1893-2002). The region is bounded by E-W trending Himalayan fold and thrust belt to the north and NNE-SSW trending Indo-Burmese orogene to the south and southeast [4]. It has produced two great earthquakes ($M \geq 8.5$), which occurred on 12 June 1897 and 15 August 1950 (Fig. 1). The entire northeastern region as a whole experienced 20 large earthquakes ($M > 7.0$) during the last 200 years [5]. This region is tectonically divided into several deep-rooted faults/thrusts along which there are reports of episodic block/thrust/strike-slip movements [6,7]. The seismicity of the northeastern region shows a higher concentration of events in the Shillong-Mikir Plateaus, Arunachal Himalaya, and Indo-Myanmar subduction zone, as shown in the tectonic map of north-east India in Fig. 1.

Various workers have investigated the seismicity of the region. In fact, from a seismotectonic perspective, the Shillong plateau and Mikir massif of northeast India is the most extensively studied regions. The Dhansiri and Kopili Faults mark the eastern and western boundary of the Mikir massif, and both have strike-slip kinematics [4] (Fig. 1).

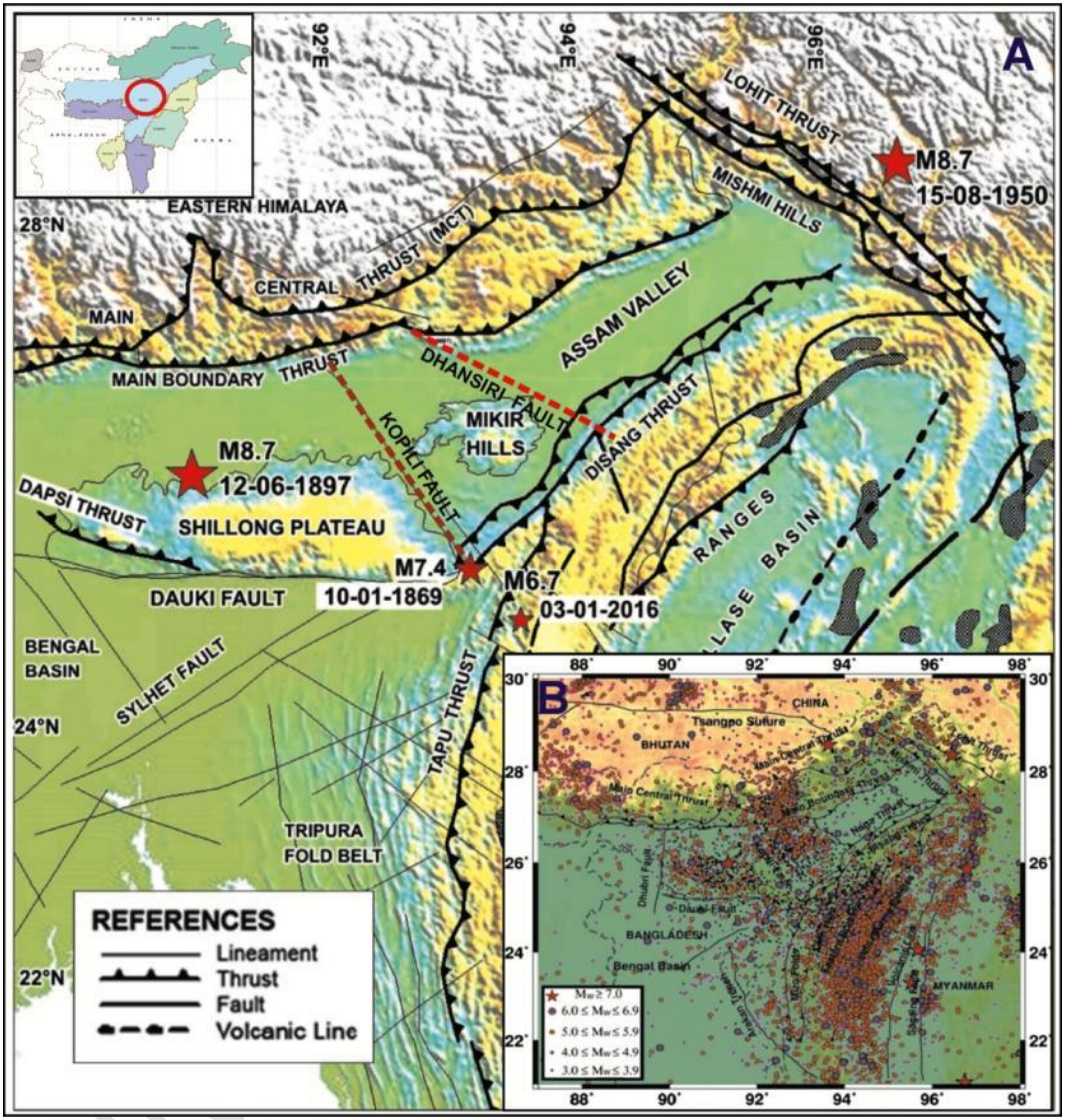

Fig.1. (A) Tectonic map of North-East India (modified after [8]) showing major thrusts, faults and lineaments, Also, past major earthquakes are shown as red colour star; (B) Seismotectonic map of Northeast India and adjoining region [9] showing the distribution of seismicity in the area.

The Mikir massif in Assam is tectonically separated from the Shillong plateau by the NW-SE trending Kopili Fault [10]. The Kopili Fault is approximately 300 km long, NW-SE trending strike-slip fault [11-13], and has a dip of 75° towards NE [4]. It is bounded by the Himalayan Fontal Thrust (HFT) to the north and by the NE-SW trending Naga Thrust to the south. Similarly, the Dhansiri Fault, also known as Bomdila-Dhansiri Fault or Dhansiri lineament [4] is a 400 km long strike-slip fault trending WNW-ESE direction and dips 50-55° towards the NNE. The Belt of Schuppen forms the eastern and southern boundaries of this fault, and the Himalayan fold belt forms its northern boundary [14]. Concentrations of higher earthquake occurrences associated with these two faults are considered to be an intraplate tectonic domain due to its complex stress regime [7,5]. The Kopili Fault has produced two large earthquakes of magnitude greater than 7 in 1869 and 1943 [4] and is thought to be responsible for the 2009 Bhutan earthquake [15]. Kayal et al., [11,16,15] have identified this region has the potential to generate future large magnitude earthquakes. The seismic hazard assessment in the northeast Indian region has been carried out by many researchers which, includes [17-23]. Thingbaijamand Nath[24]and Mohapatra et al., [25], estimated that the Shillong zone, including the Shillong plateau and Mikir massif, can generate a maximum earthquake (Mmax) of 8.7 magnitudes. In addition to these two significant faults, the region also contains three other significant geological features: the Tezpur Fault in the north, the Sarhed Fault, and the Kaliyani Lineament/Shear Zone in the central part (Fig. 2).

The present work is undertaken to study the active tectonics of the area in the Mikir massif region (Fig. 1) with the help of hypocentral parameters, frequency–magnitude relation, and b and a-value of earthquake events. The main objective of this work is to correlate the major structures and existing lineaments with the seismicity pattern of the area; to mark any possible fault by linking the earthquake epicenters to the lineament map; to study the seismotectonic activeness of the area using frequency–magnitude relation and 'b' and 'a'-value of earthquake events and finally, demarcation of the area in terms of zones from low to high seismicity and indentify those areas having low seismicity and less heterogeneity which are suitable for any civil engineering constructions.

2. Geological Settings

Geologically, the area is represented by rocks ranging in age from Archaean - Palaeoproterozoic to Recent. The oldest rock unit exposed in the Mikir massif comprises of Neoarchean-

Proterozoic to Early Paleozoic (2.6 - 0.5 Ga) basement gneissic rocks [26,27] which is represented by predominance of migmatites, quartzo-feldspathic gneisses, hornblende biotiteschists, grey and pink granitoids with irregular sporadic bodies of amphibolites representing older supracrustals[28]. These lithological assemblages collectively constitute the Assam-Meghalaya Gneissic Complex (AMGC). The AMGC is unconformably overlain by metasediments of the Shillong Group of rocks. An intra-cratonic tectonic depression had occurred during the Mesoproterozoic time followed by a sequence of deposition of thick piles of sedimentation and volcanics and subsequently metamorphosed on a regional scale. The Shillong Group of rocks of the Palaeo-mesoproterozoic age, comprising basal and intraformational conglomerate, phyllite, and quartzite, occur as basement cover rocks over the Precambrian gneisses. The Shillong Group displays multiple deformational history and metamorphism under greenschist amphibolite transitional facies [29-32]. These basement gneisses, along with the Proterozoic cover rocks, have been intruded by dolerite dykes and sills of Proterozoic age and subsequently by Neoproterozoic- Early Palaeozoicpotassic granites, pegmatites, and quartz veins. Neo-Proterozoic felsic magmatism in the Mikir massif is manifested in the form of several granitic intrusions intruded through the AMGC and overlying Meso- Proterozoic sediments of the Shillong Group. Examples of Neo- Proterozoic granites are Kathagurigranitoids and other associated granites in Dizu valley [33,26].

Following the Neo-Proterozoic felsic magmatism, there was a late phase of small-scale intrusions of dolerite and traps called Mikir trap (also known as Sylhet trap in Meghalaya) which is erratic in nature. The emplacement of the carbonatite-alkaline complex of the Cretaceous age forms the youngest igneous activity in the region [34,35]. It is represented by two complexes, namely Samchampi and Barpung. Rocks of Samchampi- Barpang Alkali Ultamafic complex of Cretaceous age and volcanic rocks as represented by Mikir Trap of Jurassice-Cretaceous age are Mesozoic thermal imprints on the Karbi- Anglong plateau. Lower Tertiary (Paleocene-Eocene) shelf sediments of the Jaintia Group extending along the southern and eastern flanks of Mikir Hills are represented by Sylhet Limestone and Sylhet Sandstone members of Shella Formation which is succeeded by KopiIi Formation of the Jaintia Group. The rocks of the Bokabil Formation of the Surma Group unconformably overlie the Jaintia Group of rocks. The upper Tertiary Neogene sequence represented by the Tipam Sandstone has been exposed at the extreme south-eastern part of the area above the Surma Group. These whole sequences are covered by alluvial soils of the Quaternary period (Fig. 2).

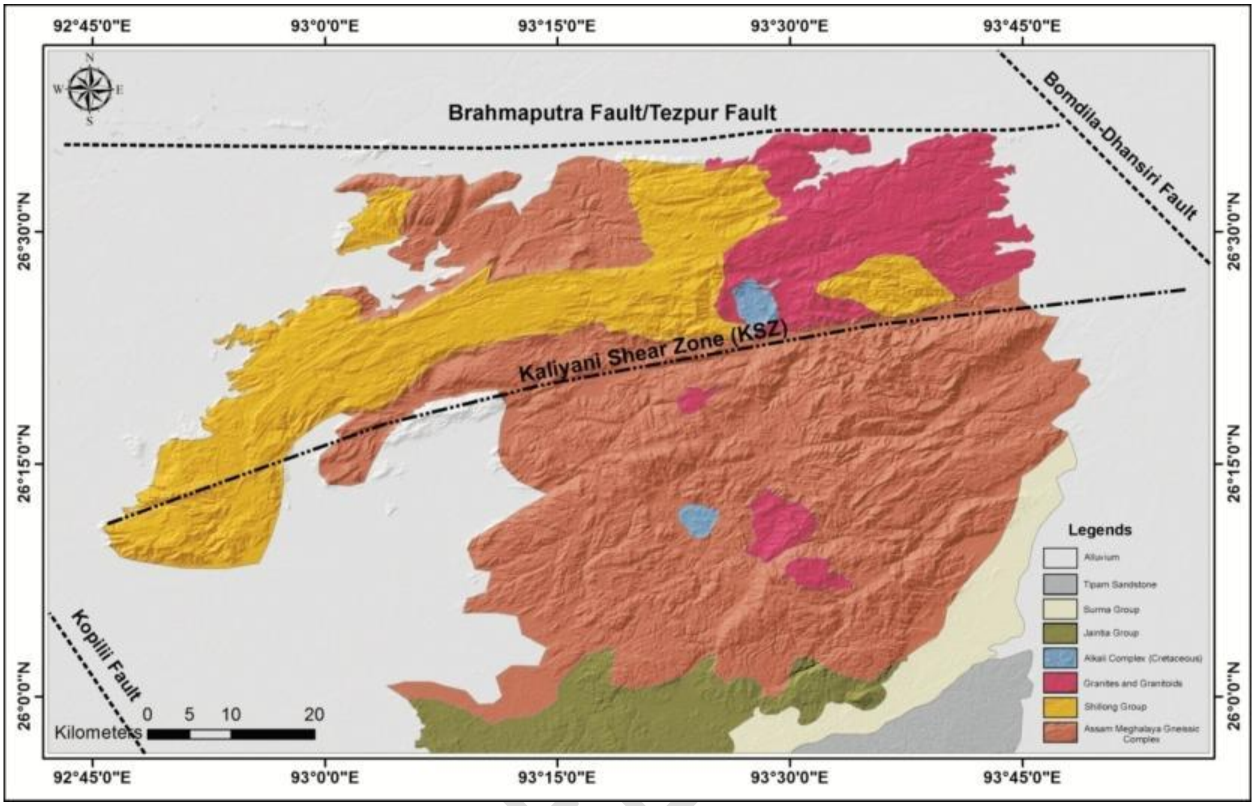

Fig. 2. A simplified geological map of the Mikir massif region showing different lithounits exposed with major faults and shear zone (after [36,37]).

3. Materials and Methods

The detailed methodology adopted in the current study has been discussed below and is shown by flow chart in Fig. 3.

3.1. Seismological dataset

A database of 1254 events consisting of hypocentral parameters such as latitude, longitude, depth (in km), and magnitude (Mw) is prepared for the period 1988 to 2013. The hypocentral database is prepared from the data collected from CSIR North East Institute of Science and Technology (NEIST), Jorhat, Assam. The whole data set comprises seismic events bounding the area with a latitude range 25°26ˈ to 27°00ˈ and longitude range 92°33ˈto 94°19ˈ occupying areas of Assam state in north and south bank of the Brahmaputra river, State of Nagaland and parts of Arunachal Pradesh (Fig. 4). For the convenience of the present study, an area of 7847 sq km, with a radius of 50 km from the center of the Mikir massif, is considered and seismic events falling within the area are used for further study. A total of 447 events for the period 1988-2013 falls within the study area (Fig. 4). The barest minimum magnitude of the earthquake events is considered to be 0.8.

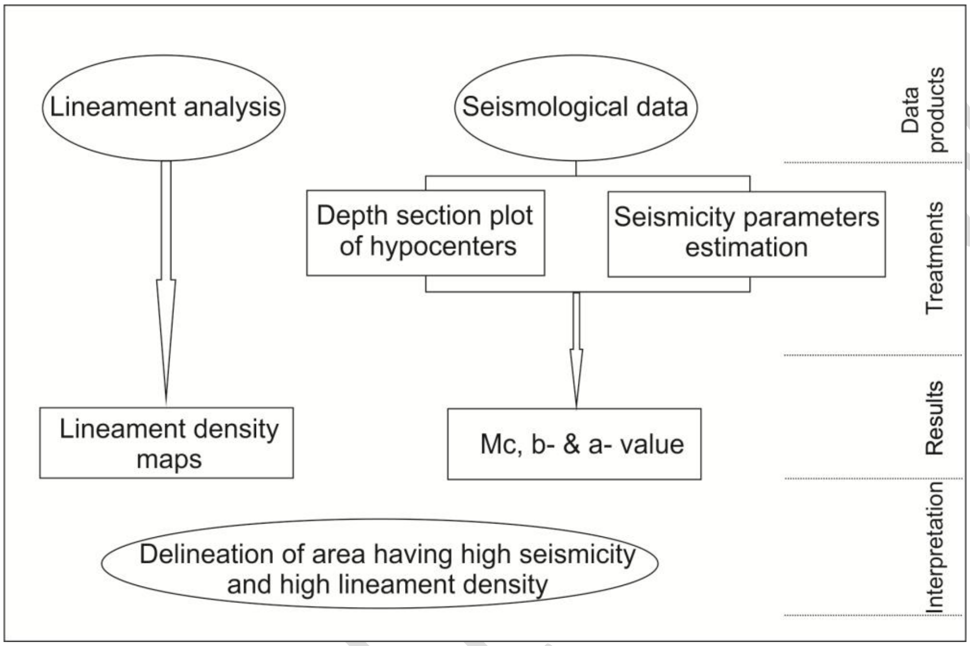

Fig. 3. Methodology flow chart of the present study.

The database seems nearly continuous, as shown in the time histogram (Fig. 5a), except for the period between the years 2005 to 2010, when no seismic events were recorded in the seismic stations. The magnitude of the earthquake events predominantly lies between 2.1 and 3.6, and the maximum concentration is noted at around 2.7 (Fig. 5b). Depth-wise distribution of seismicity beneath the study area is also significantly uneven (Fig.5c). At the shallowest level below 5 km, seismicity is significantly less, and it again drops to a minimum in the deepest part exceeding 60 km depth. Beyond 5 km, seismicity increases almost linearly and continues to a depth of 20 km. At 20 km depth, the seismicity sharply increases, with maximum concentration noted at 20 to 25 km depth. This high seismic zone has also been reported by earlier workers [38]. Thereafter, the distribution is almost uniform up to a depth of 50 km and sharply decreases till the depth of 75 km. Seismic events are nearly absent within a depth range of 75 to 85 km and 90 to 95 km, with few events in between.

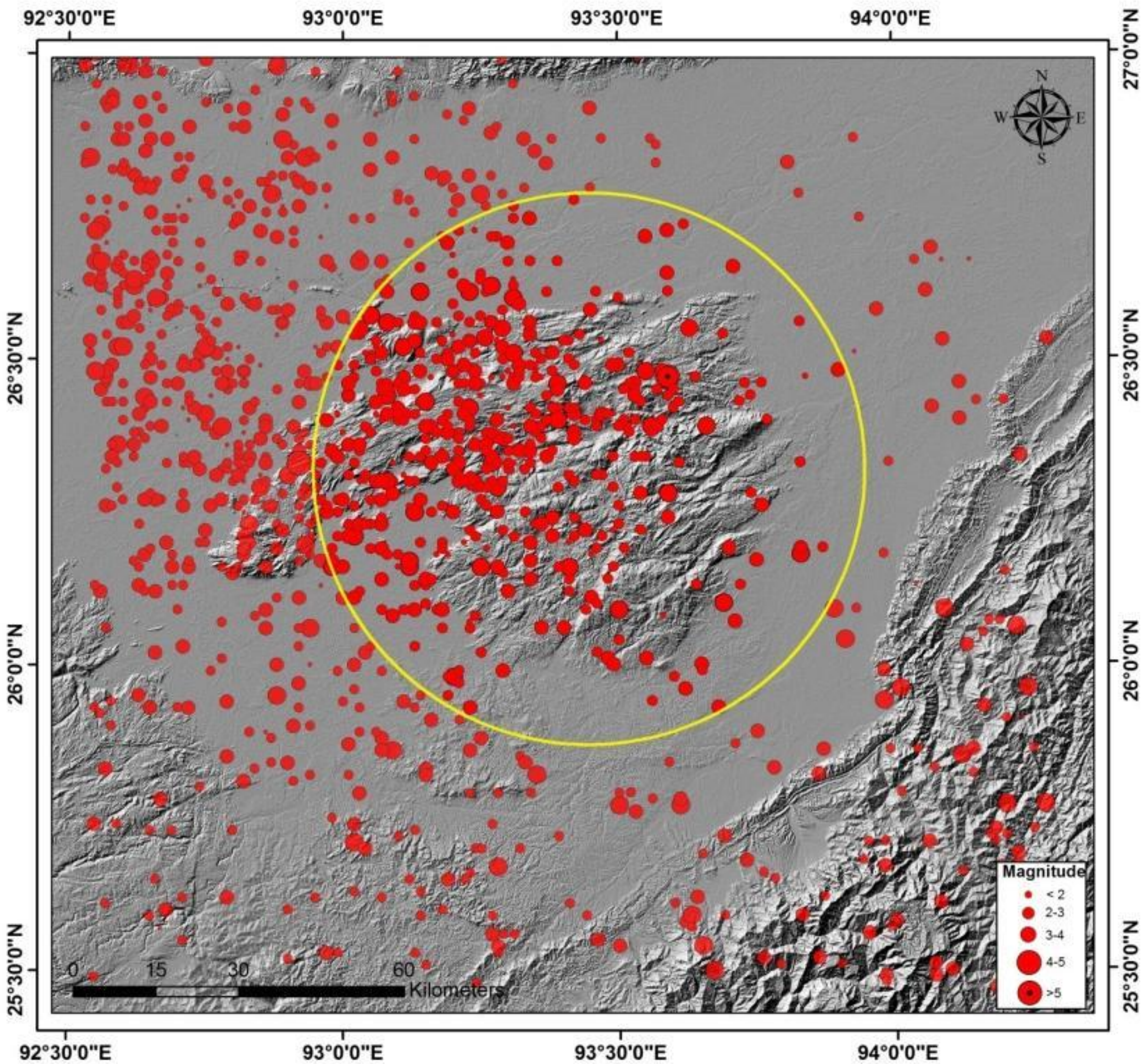

Fig. 4. Epicentral plot of available earthquake data for the period 1988-2013, collected from CSIR North East Institute of Science and Technology (NEIST), Jorhat, Assam and those fall within a radius of 50 km from the center point of Mikir massif considered for the present study.

The cumulative number of earthquakes versus time in the regions for the original catalog for the period 1988-2013 is shown in Fig. 5d. As shown in Fig. 5d, there is no significant change in reporting as a function of time between 2005 and 2010 for the region. Greater seismic changes are seen in these areas, especially after 2010. The highest magnitude event (Mw=5.5) occurred in the area on 6th November 2013 and is shown as a yellow star mark in the time series.

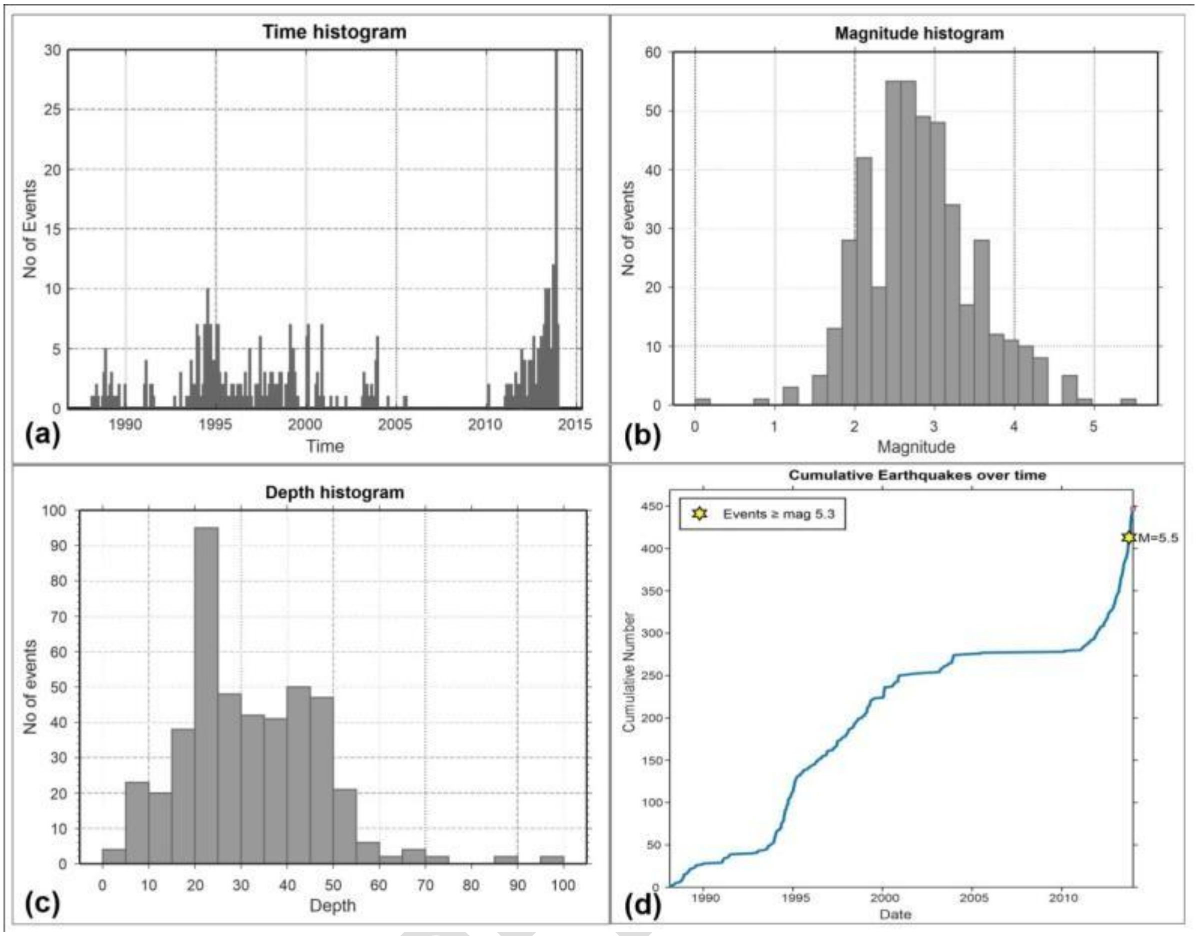

Fig. 5. Histograms illustrating concentration of seismicity with respect to time (a), magnitude (b) and depth (c) for the study area. (d) Shows the cumulative earthquake over time.

3.2. Lineament pattern of the area

Lineaments are more intense in tectonically active regions than in tectonically quiet ones. Analysis of lineaments in a region with poor exposures and dense vegetation can provide indications of tectonic activities [39]. The lineaments present in the study area have been extracted from the Landsat-8 and Digital Elevation Model (DEM) SRTM data (Fig. 7). The lineaments are then classified into two classes. Geomorphic lineaments or drainage parallel lineaments are detected on the satellite image as a straight course of streams and valleys. The structural lineaments, which are developed due to structural features such as faults, folds, cracks, or fractures were also been marked. For this purpose, the location and orientation of structural features present in the area have been consulted from the published literature available in the

Mikir massif region. Those lineaments formed due to these structural discontinuities are termed structural lineaments. Since the area is occupied by gneisses and migmatites of Archean, quartzites, and phyllites of Shillong Group, and intrusive granitoids and are highly jointed and fractured. Foliation, joints, and fractures are hence responsible for most structural lineaments. Few other lineaments that don't fall into either of these two categories but have been reported by the earlier workers in the area and have>10 km length persistence have been classified as major lineaments in the present study. Depending on their size, all major lineaments could be caused by faulting or be the surface expressions of lithological contacts [40]. The minor lineaments may be the result of joints or minor faults.

3.3. Depth section plots of hypocenters

The epicentral map utilizing the database has been plotted, covering the area between latitude 25.9°N and 26.7°N and longitude 92.9°E and 93.9°E to observe the spatial distribution of the epicenters using ArcGIS software. Fig. 6 represents the distribution of seismicity over the study area. Almost the whole area exhibit moderate to high seismic activity, with the northwestern and western parts showing the highest concentration. In other parts, particularly towards the south and southeast, the seismicity decreases phenomenally. The higher seismic activity in the south-western part compared to the north-eastern part is either due to the clockwise rotation of the Shillong plateau [41] or the counter-clockwise rotation of the Mikir block from nearly EW to NNE-SSW direction [42]. The distribution of seismicity towards the west and east, surrounding the major faults via the Kopili Fault and Dhansiri Fault, is fairly uneven. The highest magnitude event (Mw=5.5), which has been recorded in the area, is marked as an orange color star mark (Fig. 6). It occurred in the central part of the area at a depth of 51.5 km on the 6th of November, 2013.

To achieve the objective of 'classifying the area in terms of low to high seismicity', the area has been divided into four seismogenic zones viz. A, B, C, and D (Fig. 7), and seismotectonics of each zone have been accessed separately. The zones have been defined based on the incidence of the recorded earthquake and the nature and density of lineaments in the region.

In order to correlate the earthquake epicenter and the major faults and lineaments previously marked in the area, depth section plots along and across the regional structures were made.

While preparing the depth section plots, earthquakes that fall within the span of 20 km on either side of the profile lines are considered (Fig. 7).

Altogether, four depth sections are considered as follows:

a. Section A-A' (26.01°N, 93.78°E- 26.63°N, 93.12°E) along SSE-NNW direction,

b. Section B-B' (26.64°N, 93.69°E- 25.95°N, 93.10°E) along NNE-SSW direction,

c. Section C-C' (26.64°N, 93.42°E- 25.96°N, 93.44°E) along N-S direction,

These three sections are chosen across the trend of major faults, viz., Tezpur Fault, Sarhed Fault, and Kaliyani Shear Zone.

d. Section D-D' (26.47°N, 93.89°E- 26.29°N, 92.98°E) along NE-SW direction along the trend of the Kaliyani Shear Zone.

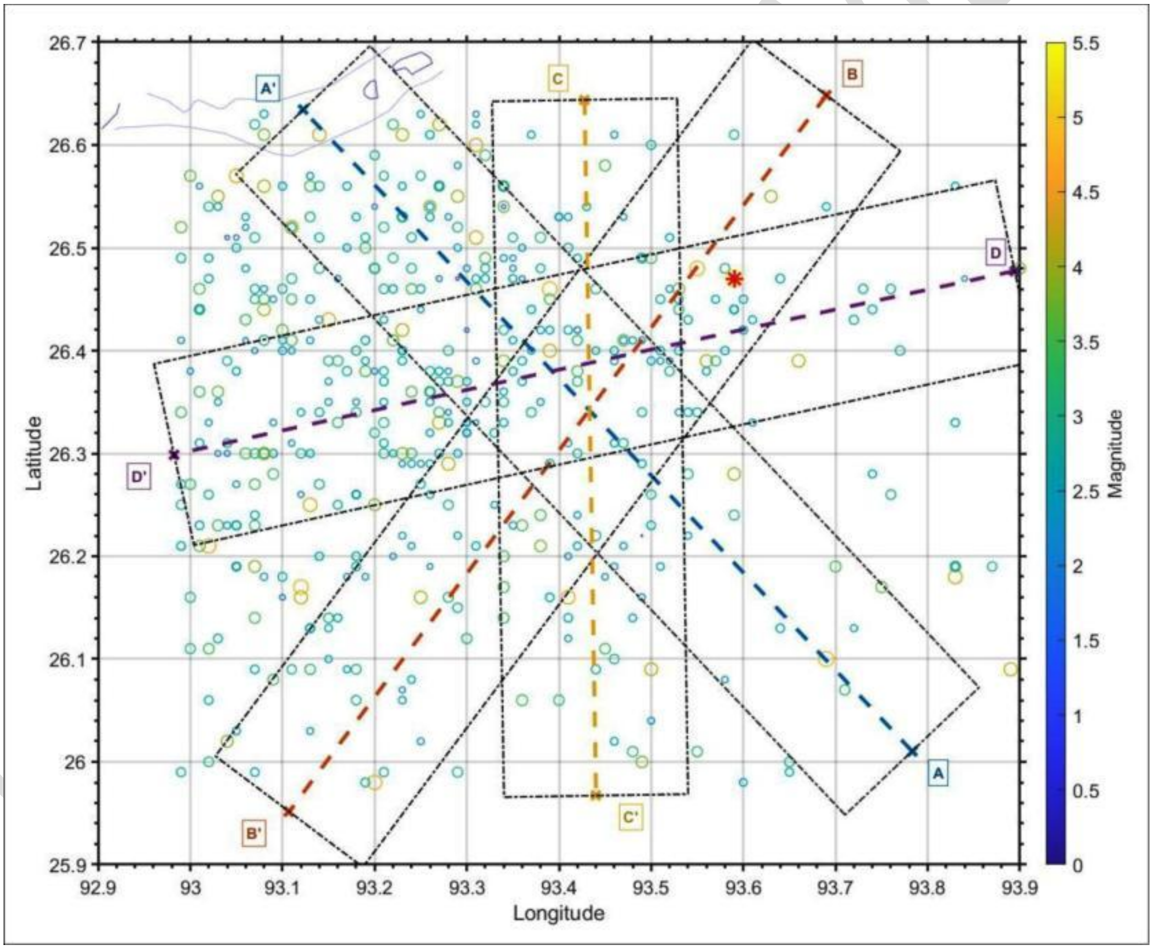

Fig. 6. Seismotectonic map of the area showing 4 numbers of section lines considered for depth vs. hypocenter plots (AA', BB', CC' and DD'). The bounding lines indicate a distance of 20 km on either side of the section lines. The orange star represents the highest magnitude event recorded in the area.

Topographic relief studies are done through topographical cross-sections along these four depth sections using the Shuttle Radar Topography Mission (SRTM) digital elevation model (DEM) available from the USGS site with a spatial resolution of 30 m. The SRTM DEM is georeferenced and projected in the UTM projection system. Fig. 7 shows the physiography map of the area with topographic relief, and Fig.8 shows the cross sections along the four profile lines with the incidence of reported earthquake events at their respective depths.The seismotectonics of the area have been inferred based primarily on the seismicity map, as shown in Fig. 7; besides depth section plots of the hypocenter along four profile lines provide an overview of seismotectonics at depth.

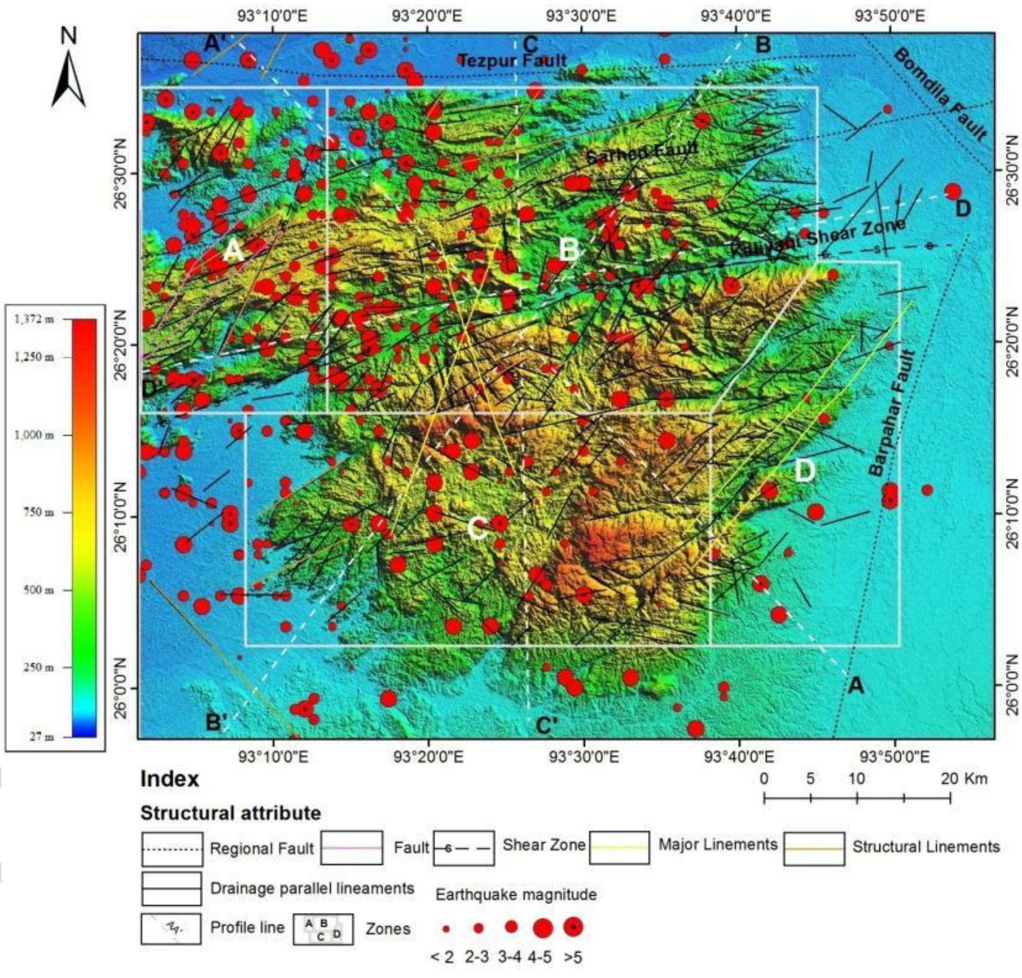

Fig. 7. Seismotectonic map of study area showing major structural discontinuity, past earthquake events and profile lines for hypocentral plot with digital elevation model showing topographic variations.

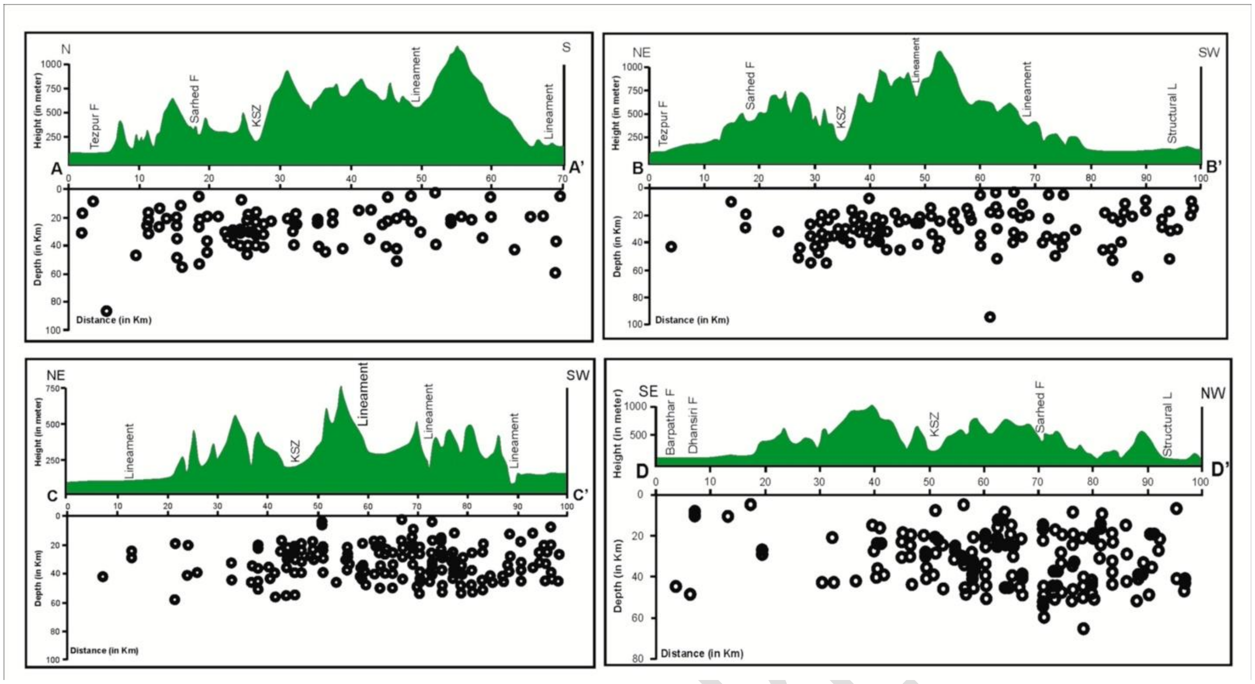

Fig. 8. Depth sections of seismic events with topographic profile along 4 sections.

3.4. Seismicity parameter estimation

The seismic activity of a region is described by two parameters that correlate between the magnitude and cumulative frequency or the rate of occurrences of a particular magnitude [1]. Gutenberg and Richter[43] developed a relationship that assumes an exponential distribution of magnitude and is expressed as:

$$\log N = a - bM \qquad \text{(Eq 1)}$$

Where 'a (intercept)' and 'b (slope)' are the constants of regression, which describe the seismicity of a region. N is the mean annual rate of occurrence of a certain magnitude Mw and above. One another important parameter is the magnitude of completeness (Mc) which is the lowest magnitude above which the earthquake recording is assumed to be complete [44].

Fig.9 shows the plot of cumulative frequency vs. magnitude, commonly known as the Frequency Magnitude Distribution (FMD) curve for the study area, showing all the parameters mentioned above and the least square fit line for which the G-R equation is valid. Again, the study area has been subdivided into four seismogenic zones keeping in view the spatial variations in earthquake occurrence and prevalent tectonics. Mc, 'b', and 'a' -values have been estimated using the G–R relationship for each zone (Fig.10), and estimated seismicity parameters are presented in Table 1.

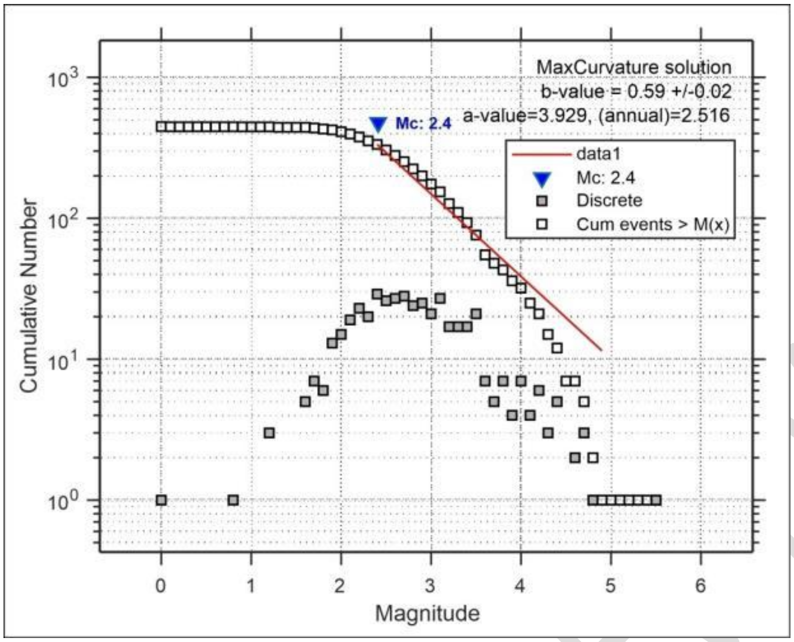

Fig. 9. Plots of cumulative frequency versus magnitude for the whole area showing ‘a’, ‘b’ and ‘Mc’ values.

Table 1 Estimation of Mc, ‘b’ and ‘a’ values for different seismogenic zones.

Seismogenic Zone	Mc	b	a
A	3.1	1.00±0.11	4.9
B	2.5	0.68±0.05	3.9
C	2.7	0.71±0.07	3.6
D	3	0.65±0.19	2.9

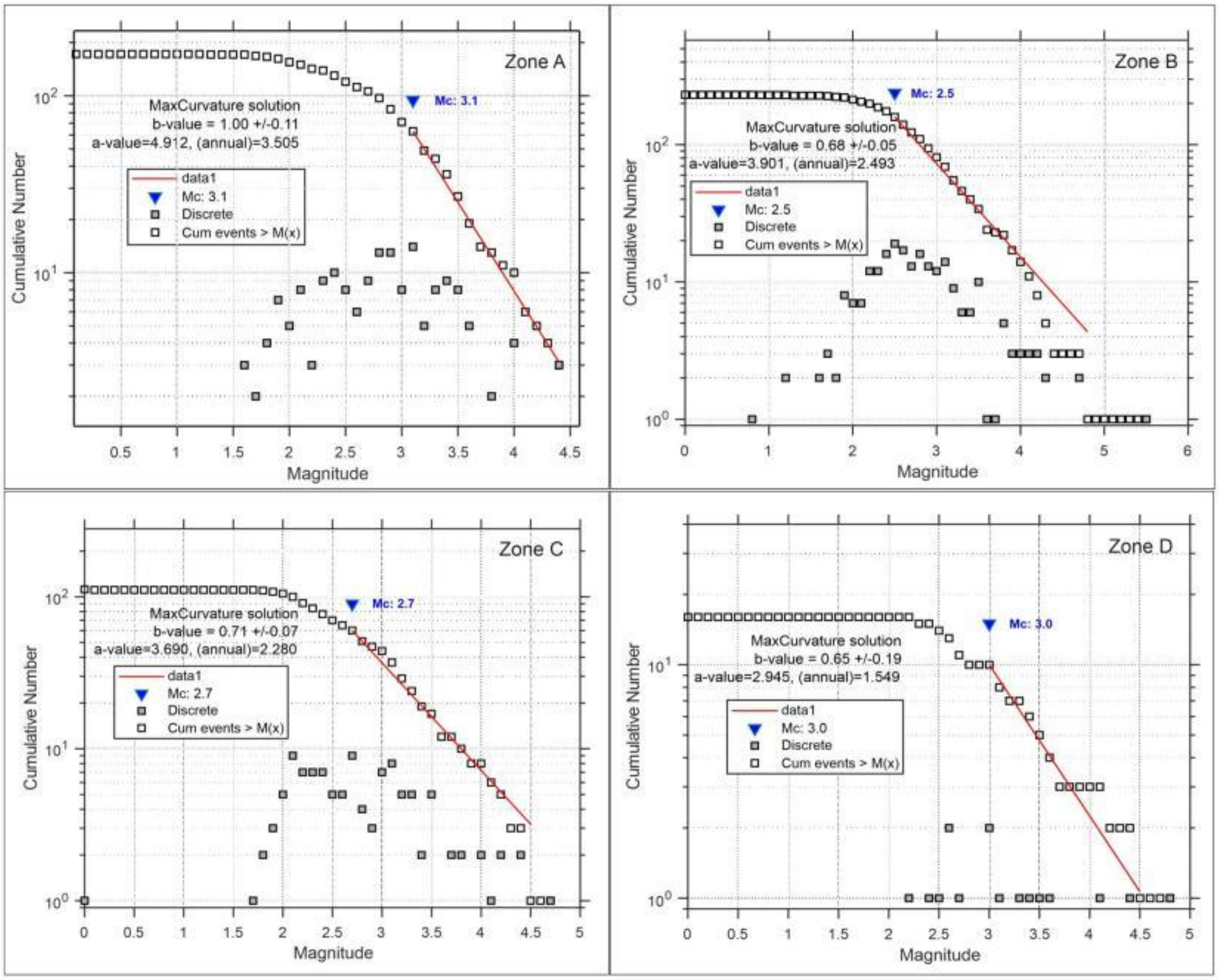

Fig. 10. Plots of cumulative frequency versus magnitude for four seismogenic zones showing 'a', 'b' and 'Mc' values.

3.4.1. Magnitude of completeness (Mc)

The magnitude of completeness (Mc), also called as 'threshold' or 'cutoff' magnitude of a seismic catalog [45], is the lowest magnitude at which 100% of the events in space and time are detected [9]. It is one of the important parameters for seismicity and seismic hazard assessment studies. Mc value defines the minimum magnitude at which the power law fits as the best fit for the FMD curve and is hence crucial for estimating a-value and b-value for hazard assessment in any tectonic regimes [9]. The magnitude of completeness can vary with time, and its value is reduced with improvement in the detection capability and/or data analysis method [46]. In this study, the Mc value is estimated from the maximum curvature of the FMD curve generated for all four seismogenic zones as proposed by Wiemer and Wyss[47].

3.4.2.'a' and 'b' value

'a' value represents the intercepts in the GR relationship for an FMD curve and indicates the seismicity level of a region. Higher'a' value indicates a higher level of seismicity. It depends on the size of the area, the observation period length, and the largest seismic magnitude recorded in an area [1]. The 'b' value, which determines the rate of fall in the frequency of events with increasing magnitude, is the slope of the regression line in the FMD curve [48]. It describes the relative size distribution of events. A high 'b' value indicates a larger proportion of smaller earthquake events [1]. High values indicate regions of low strength and large heterogeneity, whereas low values are expected in regions having high resistance and homogeneity [49-51,48]. A similar interpretation can also be applied to 'a' value variation because there is a positive relationship exists between these two parameters [52-53]. In natural situations, 'a' and 'b' values lie in the range between 2 to 8 and 0.5 to 1.8, respectively [48].

Many factors may cause the deviation of the 'b' value from a normal value of 1.0 in an active region. Increased material heterogeneity or crack density results in higher 'b' values [54], while an increase in applied shear stress decreases the 'b' value [55,56]. Its lower value is indicative of a region that is under higher shear stress, and for those areas which have already gone through the threshold stress limit, the 'b' value is generally high [57,58].

4. Results

As shown in Fig. 8, the depth section of seismic events, when combined with the topographic profile, it has been observed that all the major structures and lineaments with distinct topographic expressions can be clearly identified from the elevation profile. The cluster of seismic events occur at depth can assess the neotectonic activeness of those faults and lineaments. Again, from the spatial distribution of seismic events in Fig 7, it has been observed that many events in Zone A and Zone B aligned parallel to the existing lineaments marked in the area. Epicentral clusters have been observed mainly in zones A and west of Zone B. Therefore, it can be concluded that the majority of the lineaments and faults marked in the area are active, as evident from higher numbers of seismic activity in the recent past. To visualize the active tectonics prevailing in the area, a lineament density map has been prepared, and available earthquake records have been superimposed. The final map delineates those areas which are tectonically more active and highly fractured, marked by high to very high density of lineaments from those areas which are relatively stable with low to very low density. Fig. 11 shows the lineament density map of the study area having five classes of lineament density, viz. Very low, Low, Medium, High, and Very high.

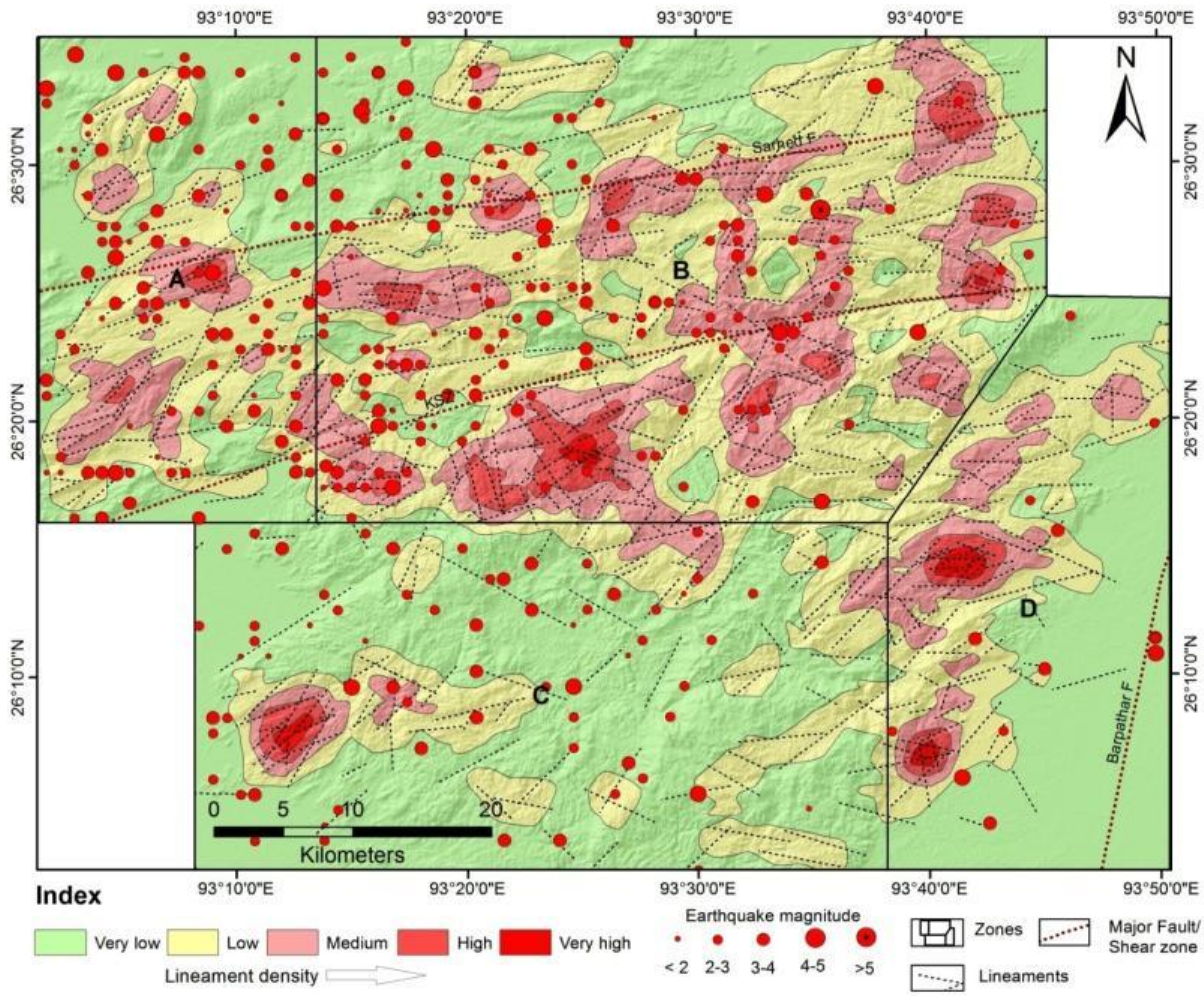

Fig. 11. Lineament density map of the area showing earthquake epicenters, all the major Faults/ Shear zone present in the area.

From Fig. 11, it has been observed that the high lineament density zones are mainly present in Zone A and Zone B in the area. In contrast, Zone D and the southeastern part of Zone C are relatively stable, having low to moderate lineament density.

From the FMD curve in Fig. 10 and Table 1, it is clear that the Zone A, is having the highest 'b' and 'a' value due to the occurrences of higher number of earthquake events having smaller magnitude. This has also been evident from the seismotectonic map of the area, as shown in Fig. 7, and the lineament density map in Fig.11. The higher b-value for this zone may also be due to higher crack density within the rocks of Gneissic complexes and Shillong Groups. The lower 'b' and 'a'- value associated with Zone D implies that the area is seismotectonically stable with fewer seismic events. To visualize the spatial distribution of Mc, 'a' and 'b'- values in the area, the study area is divided into 945 square grids for high-resolution investigation. Each grid has a dimension of 0.1°×0.1° (geographical window), corresponding to 11x11 km on the map. Fig. 12a, b & c shows the spatial distribution map for Mc, a, and b values, respectively.

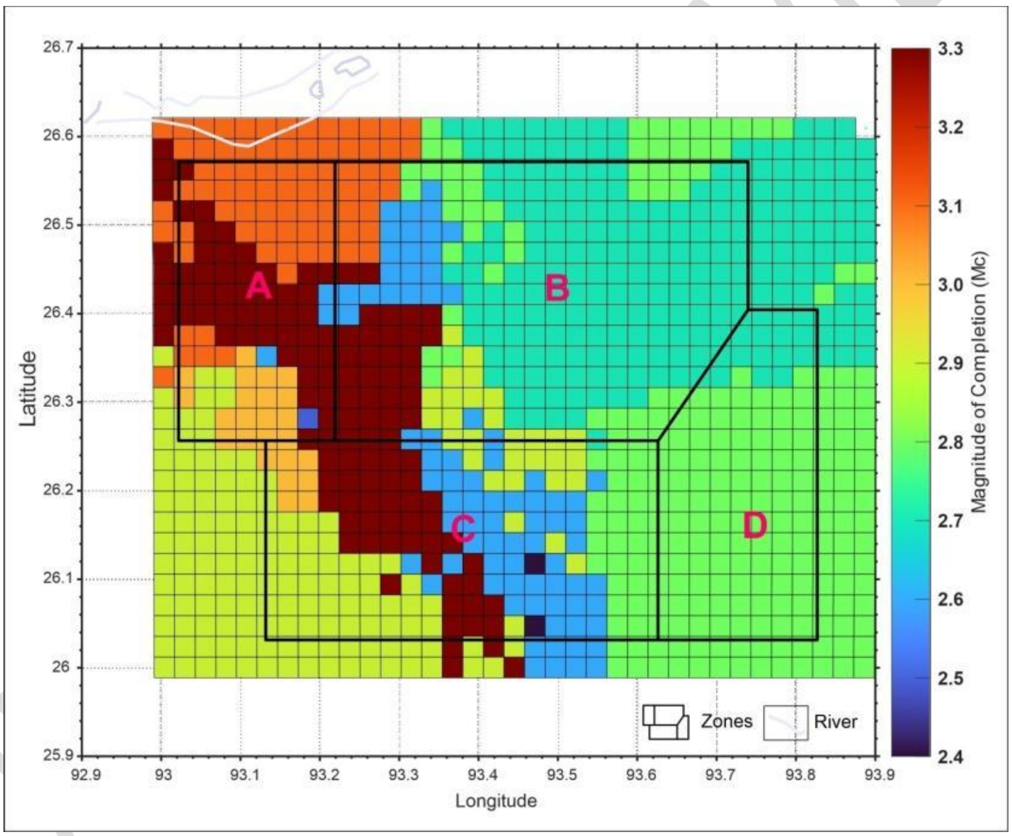

Fig. 12a. Map showing variation of Magnitude of completeness (Mc) in the study area.

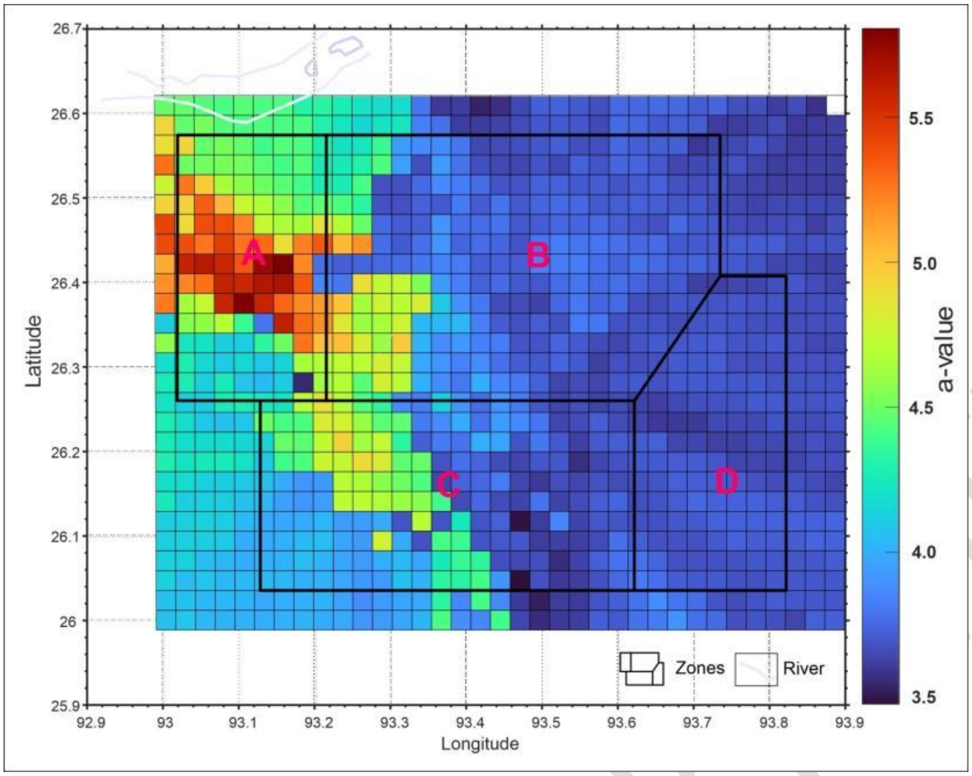

Fig. 12b. Map showing variation of a-value in the study area.

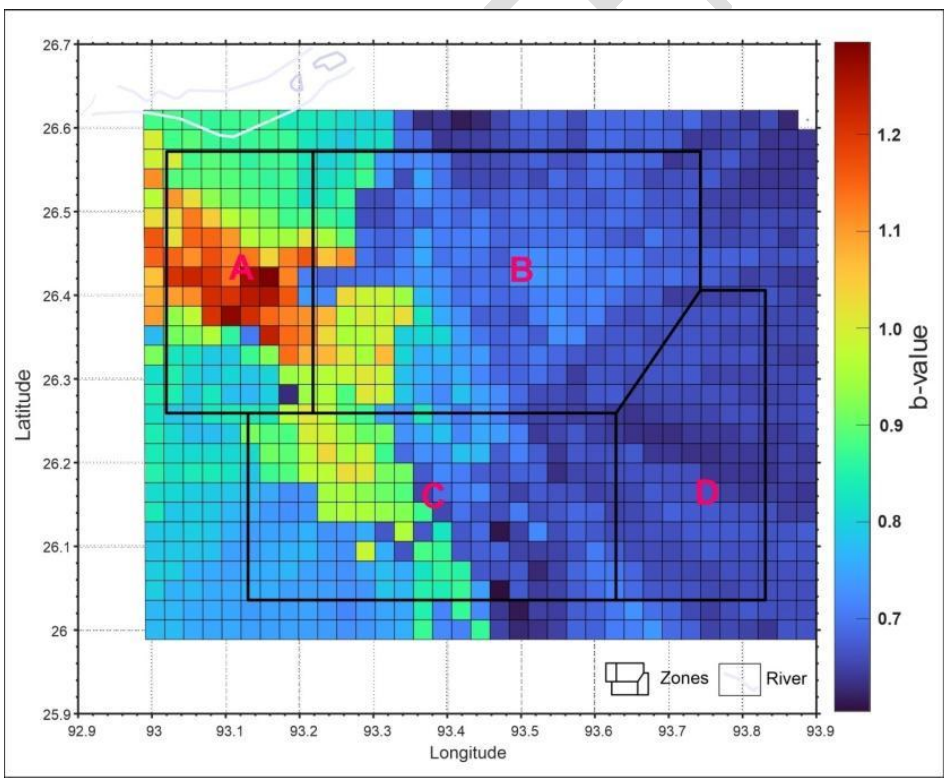

Fig. 12c. Map showing variation of b-value in the study area.

5. Discussion

From the present study, the seismotectonic scenario of tectonically active Mikir massif region of NER has been analyzed. The epicentral map of seismic events when combined with the regional structural and lineament density map of the area, it has been observed that all the high-density zones of lineament are parallel to the major fault like the Sarhed Fault, which is present in the north central part, and also to the Kaliyani Shear Zone (KSZ) in the central part of the area (Fig. 7). These are the areas of high weakness, intense fracturing, and tectonically more active in the study area. From the three seismicity parameter maps, it has been observed that Zone A is the most active zone in terms of seismicity, followed by Zone C and Zone B. A distinct linear pattern is shown by all three parameters having an NW-SE trend, covering all portions of Zone A, the western part of Zone B, and the northwest and central part of Zone C. This marks the area having the highest heterogeneity and more intense seismicity recorded in the study area. This zone represents the most tectonically active part present in the area, which may be due to the presence of deep-seated structures beneath, most likely to be a fault or shear zone which shows reactivation in the recent past. The other parts of the area, east of Zone B and C and the entire Zone D are stable, having less seismic activity. These stable regions are always suitable for any civil engineering constructions as the rock heterogeneity encountered in those areas will be significantly less compared to those with high seismicity and lineament density.

6. Conclusion

The seismicity in the area shows a higher concentration of earthquake events towards NW, compared to other parts. The northwestern part lies very close to Kopili Fault, which is most active in the NW part than in the SE part. Depth section of earthquake events coupled with topographic sections along four profiles selected along and across the regional faults shows that all the major structures and lineaments with distinct topographic expressions can be clearly identified from the elevation profile. The activeness of those faults and lineaments can be assessed by the cluster of seismic events occurring spatially and at depth. Classification of the area into four different seismogenic zones shows higher values of seismic parameters (Mc, ‘a’ and ‘b’ value) for Zone A, followed by Zone C, Zone B, and Zone D. This indicates Zone A is the most active zone due to the occurrences of higher number of earthquake events having smaller magnitude. The higher b-value for this zone may also be due to higher fracture density within the rocks of Gneissic complexes and the Shillong Group. The higher seismicity associated with these zones are also conforms with the high lineament density observed in those areas. The lower 'b' and 'a'- value associated with Zone D, implies that the area is seismotectonically stable with fewer numbers of seismic events. The spatial distribution map for Mc, a, and b value shows a distinct linear pattern having an NW-SE trend, covering all portions of Zone A, the western part of Zone B, and the northwest and central part of Zone C. This marks the area having the highest heterogeneity and more intense seismicity recorded in the study area. The other parts of the area, like, east of Zone B and C and the entire Zone D, are stable, having less seismic activity and hence suitable for any civil engineering construction.

7. References

1. Sitharam TG, Sil A. Comprehensive seismic hazard assessment of Tripura and Mizoram states. J. Earth Syst. Sci. 2014;123(4):837–857.
2. Kassaras I, Kapetanidis V, Ganas A, Tzanis A, Kosma C, Karakonstantis A, Valkaniotis S, Chailas S, Kouskouna V, Papadimitriou P. The New Seismotectonic Atlas of Greece (v1.0) and Its Implementation. Geosciences. 2020;10:447.
3. BMTPC. Vulnerability atlas, Second Edn., peer group MOH & UPA, Seismic zones of India. 2003.
4. Sharma S, Sarma JN, Baruah S. Dynamics of Mikir hills plateau and its vicinity: Inferences on Kopili and Bomdila Faults in northeastern India through seismotectonics, gravity and magnetic anomalies. Annals of Geophysics. 2018;61(3):SE338.
5. Angelier J, Baruah S. Seismotectonics of northeast India: a stress analysis if focal mechanism solutions of earthquakes and its kinematic implications. Geophysical Journal International. 2009;178(1):303-326.
6. Nandy DR. Tectonics, seismicity and gravity of Northeastern India and adjoining region. Geol. Surv. India Mem. 1986;119:13-17.
7. Nandy DR. Geodynamics of Northeastern India and the Adjoining Region: ACB Publication, Kolkata. 2001:209.
8. Kumar A, Sanoujam M, Roy LS, Kosigyn L, Singh WAR, Pandey AP. Mw 6.7 earthquake of manipur, NE India: some insights. J. Geological Soc. India. 2016;88:5–12.

9. Pandey AK, Chingtham P, Roy PNS. Homogeneous earthquake catalogue for Northeast region of India using robust statistical approaches. Geomatics, Nat. Hazards Risk. 2017;8(2):1477–1491.
10. Sarma KP, Dey T. Re-look on Shillong Plateau. Bulletin of Pure and Applied Sciences. 1996;15(2):51-54.
11. Kayal JR, Arefiev SS, Baruah S, Hazarika D, Gogoi N, Kumar A, Chowdhury SN, Kalita S. Shillong plateau earthquake in northeast India region: complex tectonic model. Current Science. 2006;91(1):109- 114.
12. Bhattacharya PM, Mukhopadhyay S, Majumdar RK, Kayal JR. 3-D seismic structure of the Northeast India region and its implications for local and regional tectonics. Journal of Asian Earth Sciences. 2008;33:25-41.
13. Bhattacharya PM, Kayal JR, Baruah S, Arefiev SS. Earthquake source zones in northeast India: seismic tomography, fractal dimension and b-value mapping. Pure and Applied Geophysics. 2010: DOI: 10.1007/s00024-010-0084-2.
14. Nandy DR, Dasgupta S. Seismotectonic domain of northeastern India and adjacent areas. Physics and Chemistry of the Earth. 1991;18:371-384.
15. Kayal JR, Arefiev SS, Baruah S, Hazarika D, Gogoi N, Gautam JL, Baruah S, Dorbath C, Tatevossian R. Large and great earthquakes in the Shillong plateau-Assam valley area of Northeast India Region: Pop-up and transverse tectonics. Tectonophysics. 2012;532:186-192.
16. Kayal JR, Arefiev SS, Baruah S, Tatevossian R, Gogoi N, Sanoujam M, Gautam JL, Hazarika D, Borah D. The 2009 Bhutan and Assam felt earthquakes (Mw 6.3 and 5.1) at the Kopili fault in the northeast Himalaya region. Geomatics Natural Hazards and Risk. 2010;1(3):273-281.
17. Shanker D, Sharma ML. Estimation of Seismic Hazard Parameters for the Himalayas and its Vicinity from complete data files. Pure &Appld. Geophys. 1998;152(2):267–279.
18. Parvez IA, Ram A. Probabilistic assessment of earthquake hazards in the Indian Subcontinent. Pure Appld. Geophys. 1999;154(1):23–40.
19. Shanker D, Papadimitriou EE. Regional time predictable modeling in Hindukush-Pamir-Himalayas region. Tectonophysics. 2004;390:129–140.

20. Tripathi JN. Probabilistic assessment of earthquake recurrence in the January 26, 2001 earthquake region of Gujarat, India. Jour. Seism. 2006;10:119–130.
21. Mohanty WK, Walling MY. Seismic hazard in mega city Kolkata, India. Natural Hazards. 2008a;47:39–54.
22. Mohanty WK, Walling MY. First Order Seismic Microzonation of Haldia, Bengal Basin (India) Using a GIS Platform. Pure Appld. Geophys. 2008b;165:1325–1350.
23. Mohanty WK, Walling MY. An overview on the seismic zonation and microzonation studies in India. Earth Sci. Rev. 2009;96(1-2):67–91.
24. Thingbaijam KKS, Nath SK. Estimation of maximum earthquakes in northeast India. Pure and Applied Geophysics. 2008;165(5):889 –901.
25. Mohapatra AL, Mohanty WK, Verma AK. Estimation of maximum magnitude (Mmax): Impending large earthquakes in northeast region, India. Jour. Geol. Soc. India. 2014;83(6):635-640.
26. Majumdar D, Dutta P. Geodynamic evolution of a Pan-African granitoid of extended Dizo Valley in Karbi Hills, NE India: Evidence from Geochemistry and Isotope Geology. Journal of Asian Earth Sciences. 2016;117:256–268.
27. Kumar S, Rino V, Hayasaka Y, Kimura K, Raju S, Terada K, Pathak M. Contribution of Columbia and Gondwana Supercontinent assembly and growth-related magmatism in the evolution of Meghalaya Plateau and the Mikir Hills, Northeast India: constraints from U-Pb SHRIMP zircon geochronology and Geochemistry. Lithos. 2017;277:356-375.
28. Dutta JC, Chowdhury S, Das DP, Sharma SN, Bora A, Sarmah GC. Geology of parts of KarbiAnglong, North Cachar Hills and Nagaon Districts, Assam. Unpublished progress report of GSI. 1993;FS: 1991-92.
29. Mitra SK. Polydeformation of rocks of Shillong group around Sohiong, East Khasi Hills. Indian Journal of Geology. 1989;70(1&2):123-131.
30. Devi NR, Sarma KP. Strain Analysis and Stratigraphic Status of Nongkhya, Sumer and Mawmaram Conglomerates of Shillong basin of Meghalaya, India. Journal of Earth System Science. 2010;119(2):161-174.
31. Sarma KP, Ahmed M, Goswami TK. Strain analysis of the Nongkhya conglomerate. Indian Minerals. 2001;55(3&4):227-236.

32. Sarma KP, Venkateshwarlu M, Patil SK, Laskar JJ, Devi NR, MallikharjunaRao J. Palaeomagnetic study of Metadolerite dykes and sills from Proterozoic Shillong Basin, NE India. Journal of Geological Society of India. 2014;83(2):147-155.
33. Majumdar D, Dutta P. Rare earth element abundances in some A-type Pan-African granitoids of Karbi Hills, North East India. Current Science. 2014;107(12):2023–2029.
34. Pancholi GK, Chandra Sekhar DR. A report on geological traverse across Mikir Hills, KarbiAnglong Dist., Assam. Unpublished progress report of GSI. 1979;FS: 1978-79.
35. Nag S, Sengupta SK, Gaur RK, Absar A. Alkaline rocks of Samchampi-Samteran, District KarbiAnglong, Assam, India. Proc. Indian Acad. Sci. (Earth Planet. Sci.). 1999;108(1):33-48.
36. GSI. Seismotectonic Atlas of India and its Environs. Geol. Surv. India Pub. 2000:86-111.
37. GSI. Geology and mineral resources of Assam. Geological Survey of India, Miscellaneous Publication. 2009;30(IV):2(i).
38. Baruah S, Duarah R, Yadav DK. Pattern of Seismicity in ShillongMikir Plateau and the orientation of compressional axis. Journal of Geological Society of India. 1997;49:533-538.
39. Mahanta BN, Syngai BR, Srikarni C, Ahmed M. Manual Extraction and Integration of Lineament Indices for Lineament Analysis in Parts of Lower Dibang Valley, Lohit and Anjaw Districts, Arunachal Pradesh. Journal of Earth Science, Special volume. 2013:142-150.
40. Bakliwal PC, Ramasamy SM. Lineament Fabric of Rajasthan and Gujarat, India. Rec. Geol. Surv. India (Jaipur). 1987;113(7):54-64.
41. Duarah BP, Phukan S. Understanding the tectonic behaviour of the Shillong Plateau, India. J. Geol. Soc. India. 2011;77(2):105–112.
42. Dutta TK. Seismicity of Assam in Relation to Geotectonic Processes- Nature of Instability of the Assam Wedge. Bull. Int. Inst. Sets. and Earth. Eng. 1967;4:63.
43. Gutenberg B, Richter CF. Seismicity of the Earth, second ed., Princeton University Press, Princeton. 1954. https://authors.library.caltech.edu/45746/1/Gutenberg_1941p1.pdf.
44. Rydelek PA, Sacks IS. Testing the completeness of earthquake catalogs and the hypothesis of self-similarity. Nature. 1989;337(6204):251–253.

45. Woessner J, Wiemer S. Assessing the quality of earthquake catalogues: Estimating the magnitude of completeness and its uncertainty. Bull. Seismol. Soc. Am. 2005;95(2):684–698.
46. Das R, Wason HR, Sharma ML. Temporal and spatial variations in the magnitude of completeness for homogenized moment magnitude catalog for Northeast India. J. Earth Syst. Sci. 2012;121(1):19–28.
47. Wiemer S, Wyss M. Minimum magnitude of complete reporting in earthquake catalogs: examples from Alaska, the western United States and Japan. Bull. Seismol. Soc. Am. 2000;90(4):859–869.
48. Khan PK, Ghosh M. Srivastava VK. Seismic a-value and the Spatial Stress-Level Variation in Northeast India. J. Ind. Geophys. Union. 2009;13(2):49-62.
49. Tsapanos TM. b-values of two tectonic parts in the Circum-Pacific belt. Pure & App. Geophys. 1990;134(2):229- 242.
50. Wason HR, Sharma ML, Khan PK, Kapoor K, Nandini D, Kara V. Analysis of aftershocks of the Chamoli Earthquake of March 29, 1999 using broadband seismic data. J. Him. Geol. 2002;23:7-18.
51. Khan PK. Study of the occurrence of two recent damaging earthquakes and their aftershocks in the Central Himalaya. In National Symposium on Developments in Geophysical Sciences in India, BHU, Varanasi (extended abstract). 2003:114116.
52. Kaila KL, Narain H. A new approach for preparation of quantitative seismicity maps applied to Alpide belt-Sunda arc and adjoining areas. Bull. Seism. Soc. Am. 1971;61(5):1275-1291.
53. Kaila KL, MadhavaRao N, Narain H. Seismotectonic maps of southwest Asia region comprising Eastern Turkey, Caucasus, Persian Plateau, Afghanistan and Hindukush. Bull. Seism. Soc. Am. 1974;64(3-1):657-669.
54. Sharma S, Baruah S, Sahu OP, Bora PK, Duarah R. Low b-value prior to the Indo-Myanmar subduction zone earthquakes and pre-cursory swarm before the May 1995 M 6.3 earthquake. Journal of Asian Earth Sciences. 2013;73:176-183.
55. Scholz CH. The frequency-magnitude relation of microfacturing in rock and its relation to earthquakes. Bull. Seism. Soc. Am. 1968;58(1): 399-415.

56. Kayal JR. Microearthquake Seismology and Seismotectonics of South Asia, Springer. 2008;503:273–275.

57. Singh C, Bhattacharya PM, Chadha RK. Seismicity in Koyna-Warna reservoir site in Western India: fractal and b-value mapping. Bulletin of the Seismological Society of America. 2008;98(1):476–482.

58. Bhattacharya M, Kayal JR, Baruah S, Arefiev SS. Earthquake source zones in northeast India: seismic tomography, fractal dimension and b-value mapping. In Seismogenesis and earthquake forecasting, The Frank Evison volume II, Springer, Basel. 2010:145-158. DOI: 10.1007/978-3-0346-0500-7_11.